

# Top quark FCNC decays and productions at LHC in littlest Higgs model with T-parity

Xiao-Fang Han, Lei Wang, Jin Min Yang

*Key Laboratory of Frontiers in Theoretical Physics,*

*Institute of Theoretical Physics, Academia Sinica, Beijing 100190, China*

## Abstract

In the littlest Higgs model with T-parity (LHT) the newly introduced mirror quarks have flavor-changing couplings with the Standard Model (SM) quarks and may enhance the flavor-changing neutral-current (FCNC) top quark interactions which are extremely suppressed in the SM. In this work we perform a comprehensive study for the contributions of these mirror fermions to various top quark FCNC decays and productions at the LHC, which includes the decays  $t \rightarrow cV (V = g, \gamma, Z)$ ,  $t \rightarrow cgg$  and the productions proceeding through the parton processes  $cg \rightarrow t$ ,  $gg \rightarrow t\bar{c}$ ,  $cg \rightarrow tg$ ,  $cg \rightarrow t\gamma$  and  $cg \rightarrow tZ$ . We find that although these FCNC processes can be greatly enhanced by the LHT contributions, they are hardly accessible at the LHC. Therefore, the LHT model may not cause the FCNC problem in the top quark sector if the top quark property is proved to be SM-like at the LHC.

PACS numbers: 14.80.Cp, 12.60.Fr, 11.30.Qc

## I. INTRODUCTION

As a possible solution to the hierarchy problem, the little Higgs theory was proposed [1] and so far remains a popular candidate for new physics beyond the Standard Model (SM). The littlest Higgs model [2] is a cute economical implementation of the little Higgs idea, but is found to be subject to strong constraints from electroweak precision tests [3], which would require raising the mass scale of the new particles to far above TeV scale and thus reintroduce the fine-tuning in the Higgs potential [4]. To tackle this problem, a discrete symmetry called T-parity is proposed [5], which forbids the tree-level contributions from the heavy gauge bosons to the observables involving only SM particles as external states. With the running of the LHC, these little Higgs models will soon be put to the test. To unravel the hints of these models, the Higgs boson processes may be of primary importance because these models significantly alter the property of the Higgs boson [6].

Another sensitive probe for new physics like these little Higgs models is the top quark processes. As the heaviest known elementary particle, top quark may be a window to look into the TeV-scale physics. So far the top quark properties have not been precisely measured at the Tevatron collider due to the small statistics and there remains plenty of room for new physics in the top quark sector. As a top quark factory, the LHC will allow to scrutinize the top quark nature, which may provide clues to new physics [7]. For the little Higgs model with T-parity (LHT), one aspect of its phenomenology in top quark sector is that the newly introduced mirror quarks have flavor-changing couplings with the SM quarks and may enhance the flavor-changing neutral-current (FCNC) top quark interactions which are extremely suppressed in the SM [8]. Just like their effects in the rare decays of  $K$  and  $B$  mesons [9, 10, 11] as well as in the rare decays of the Higgs and  $Z$  bosons [12], their contributions to various top quark FCNC decays and productions at the LHC may be significant and should be seriously checked.

In this work we collectively study the LHT contributions to the top quark FCNC decays and productions at the LHC, which includes the decay modes  $t \rightarrow cV (V = g, \gamma, Z)$ ,  $t \rightarrow cgg$  and the productions proceeding through the parton processes  $cg \rightarrow t$ ,  $gg \rightarrow t\bar{c}$ ,  $cg \rightarrow tg$ ,  $cg \rightarrow t\gamma$  and  $cg \rightarrow tZ$ . Some of these processes have been studied in the literature [13, 14], while the decay  $t \rightarrow cgg$  and the production  $cg \rightarrow t$  have not yet been considered. As found in other new physics models, like the supersymmetric models [15] and the technicolor models

[16], these two channels have the largest rates among the FCNC top quark processes. On the other hand, the contributions of box diagrams, which are not included in the calculations in the literature, should also be considered because their contributions to the productions are at the same order as the vertex loops. Further, since all these decays and productions depend on a same set of parameters and are strongly correlated, they should be studied and displayed collectively and comparatively.

The work is organized as follows. In Sec. II we recapitulate the LHT model and discuss the new flavor violating interactions which will contribute to the FCNC processes considered in this work. In Sec. III we calculate the LHT contributions to the top quark FCNC processes and present some numerical results. Finally, we give our conclusions in Sec. IV.

## II. THE LITTLEST HIGGS MODEL WITH T-PARITY

The LHT model [5] is based on a non-linear sigma model describing the spontaneous breaking of a global  $SU(5)$  down to a global  $SO(5)$  by a  $5 \times 5$  symmetric tensor at the scale  $f \sim \mathcal{O}(\text{TeV})$ . From the  $SU(5)/SO(5)$  breaking, there arise 14 Goldstone bosons which are described by the "pion" matrix  $\Pi$ , given explicitly by

$$\Pi = \begin{pmatrix} -\frac{\omega^0}{2} - \frac{\eta}{\sqrt{20}} & -\frac{\omega^+}{\sqrt{2}} & -i\frac{\pi^+}{\sqrt{2}} & -i\phi^{++} & -i\frac{\phi^+}{\sqrt{2}} \\ -\frac{\omega^-}{\sqrt{2}} & \frac{\omega^0}{2} - \frac{\eta}{\sqrt{20}} & \frac{v+h+i\pi^0}{2} & -i\frac{\phi^+}{\sqrt{2}} & \frac{-i\phi^0+\phi^P}{\sqrt{2}} \\ i\frac{\pi^-}{\sqrt{2}} & \frac{v+h-i\pi^0}{2} & \sqrt{4/5}\eta & -i\frac{\pi^+}{\sqrt{2}} & \frac{v+h+i\pi^0}{2} \\ i\phi^{--} & i\frac{\phi^-}{\sqrt{2}} & i\frac{\pi^-}{\sqrt{2}} & -\frac{\omega^0}{2} - \frac{\eta}{\sqrt{20}} & -\frac{\omega^-}{\sqrt{2}} \\ i\frac{\phi^-}{\sqrt{2}} & \frac{i\phi^0+\phi^P}{\sqrt{2}} & \frac{v+h-i\pi^0}{2} & -\frac{\omega^+}{\sqrt{2}} & \frac{\omega^0}{2} - \frac{\eta}{\sqrt{20}} \end{pmatrix}. \quad (1)$$

Under T-parity the SM Higgs doublet  $H = (-i\pi^+/\sqrt{2}, (v+h+i\pi^0)/2)^T$  is T-even while other fields are T-odd. A subgroup  $[SU(2) \times U(1)]_1 \times [SU(2) \times U(1)]_2$  of the  $SU(5)$  is gauged and at the scale  $f$  it is broken into the SM electroweak symmetry  $SU(2)_L \times U(1)_Y$ . The Goldstone bosons  $\omega^0$ ,  $\omega^\pm$  and  $\eta$  are respectively eaten by the new T-odd gauge bosons  $Z_H$ ,  $W_H$  and  $A_H$ , which obtain masses at  $\mathcal{O}(v^2/f^2)$

$$M_{W_H} = M_{Z_H} = fg \left(1 - \frac{v^2}{8f^2}\right), \quad M_{A_H} = \frac{fg'}{\sqrt{5}} \left(1 - \frac{5v^2}{8f^2}\right), \quad (2)$$

with  $g$  and  $g'$  being the SM  $SU(2)$  and  $U(1)$  gauge couplings, respectively.

The Goldstone bosons  $\pi^0$  and  $\pi^\pm$  are eaten by the T-even  $Z$  and  $W$  bosons of the SM, which obtain masses at  $\mathcal{O}(v^2/f^2)$

$$M_{W_L} = \frac{gv}{2} \left(1 - \frac{v^2}{12f^2}\right), \quad M_{Z_L} = \frac{gv}{2 \cos \theta_W} \left(1 - \frac{v^2}{12f^2}\right). \quad (3)$$

The photon  $A_L$  is also T-even and remains massless.

For each SM quark, a copy of mirror quark with T-odd quantum number is added in order to preserve the T-parity. We denote them by  $u_H^i$  and  $d_H^i$ , where  $i = 1, 2, 3$  are the generation index. In  $\mathcal{O}(v^2/f^2)$  their masses are given by

$$m_{d_H^i} = \sqrt{2}\kappa_{q^i} f, \quad m_{u_H^i} = m_{d_H^i} \left(1 - \frac{v^2}{8f^2}\right), \quad (4)$$

where  $\kappa_{q^i}$  are the diagonalized Yukawa couplings of the mirror quarks.

Note that new flavor interactions arise between the mirror fermions and the SM fermions, mediated by the T-odd gauge bosons or T-odd Goldstone bosons. In general, besides the charged-current flavor-changing interactions, the FCNC interactions between the mirror fermions and the SM fermions can also arise from the mismatch of rotation matrices. For example, there exist FCNC interactions between the mirror up-type (down-type) quarks and the SM up-type (down-type) quarks, where the mismatched mixing matrix is denoted by  $V_{H_u}$  ( $V_{H_d}$ ) with  $V_{H_u}^\dagger V_{H_d} = V_{CKM}$ . We follow [17] to parameterize  $V_{H_d}$  with three angles  $\theta_{12}^d, \theta_{23}^d, \theta_{13}^d$  and three phases  $\delta_{12}^d, \delta_{23}^d, \delta_{13}^d$

$$\begin{pmatrix} c_{12}^d c_{13}^d & s_{12}^d c_{13}^d e^{-i\delta_{12}^d} & s_{13}^d e^{-i\delta_{13}^d} \\ -s_{12}^d c_{23}^d e^{i\delta_{12}^d} - c_{12}^d s_{23}^d s_{13}^d e^{i(\delta_{13}^d - \delta_{23}^d)} & c_{12}^d c_{23}^d - s_{12}^d s_{23}^d s_{13}^d e^{i(\delta_{13}^d - \delta_{12}^d - \delta_{23}^d)} & s_{23}^d c_{13}^d e^{-i\delta_{23}^d} \\ s_{12}^d s_{23}^d e^{i(\delta_{12}^d + \delta_{23}^d)} - c_{12}^d c_{23}^d s_{13}^d e^{i\delta_{13}^d} & -c_{12}^d s_{23}^d e^{i\delta_{23}^d} - s_{12}^d c_{23}^d s_{13}^d e^{i(\delta_{13}^d - \delta_{12}^d)} & c_{23}^d c_{13}^d \end{pmatrix}. \quad (5)$$

### III. FCNC TOP QUARK PROCESSES IN THE LHT MODEL

The LHT contributions to the FCNC top quark processes come from the interactions between the SM quarks and the T-odd mirror quarks, mediated by the heavy T-odd gauge bosons or Goldstone bosons. The relevant Feynman diagrams for the LHT contributions are shown in Figs. 1-3. The Feynman diagrams for  $cg \rightarrow t$ ,  $gg \rightarrow t\bar{c}$  and  $cg \rightarrow tg$  are similar to Figs. 1-3 and not plotted here.

The calculations of the loop diagrams are straightforward. Each loop diagram is composed of some scalar loop functions [18], which are calculated by using LOOPTOOLS [19]. The

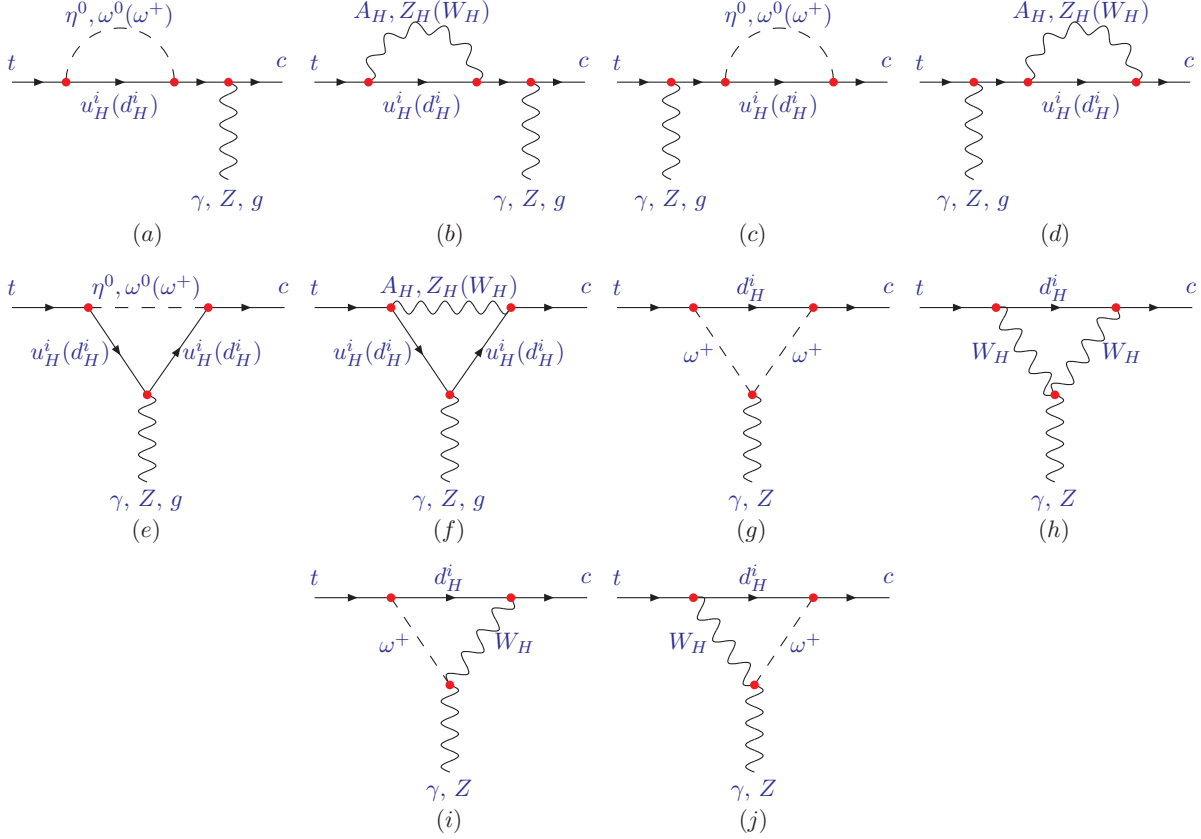


FIG. 1: Feynman diagrams for  $t \rightarrow cV$  ( $V = g, \gamma, Z$ ) at one-loop level in the LHT model.

relevant Feynman rules can be found in [11]. The analytic expressions of the amplitudes for these processes are lengthy and tedious. Here, as an example, we list the expressions for the amplitudes of  $t \rightarrow cg$  and  $t \rightarrow cgg$  in Appendix A. Note that we have checked that the divergences are canceled at  $\mathcal{O}(v^2/f^2)$  for all the processes except the channel  $t \rightarrow cZ$ . This so-called left-over divergence in the LHT model was understood as the sensitivity of the decay amplitudes to the ultraviolet completion of the theory [11]. In our numerical calculations, we will follow [11] to remove the divergent term  $1/\varepsilon$  and take the renormalization scale  $\mu = \Lambda$  with  $\Lambda = 4\pi f$  being the cutoff scale of the LHT model. Note that in [20] the similar divergence in the processes with down-type quarks or leptons as the external particles can be cancelled via the modified interactions of the up-type mirror fermions with the  $Z$  boson. We checked that such a modification cannot lead to the cancellation of the divergence in  $t \rightarrow cZ$ .

In our numerical calculations we take the SM parameters as  $m_t = 171.4$  GeV,  $m_Z = 91.187$  GeV,  $m_W = 80.425$  GeV,  $m_c = 1.25$  GeV,  $\alpha = 1/128$  and  $\alpha_s = 0.107$ . The LHT parameters relevant to our study are the scale  $f$ , the mirror quark masses and parameters

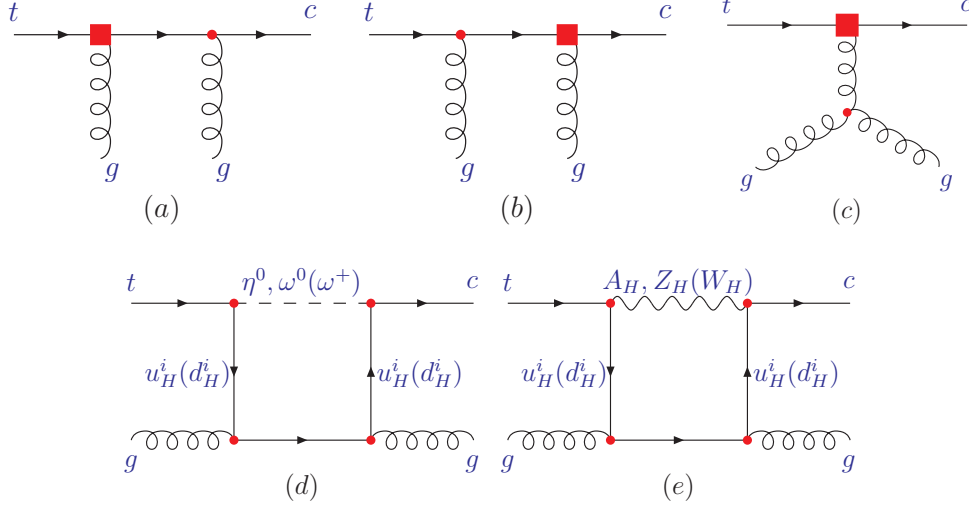


FIG. 2: Feynman diagrams for  $t \rightarrow cgg$  at one-loop level in the LHT model. The loop-induced  $tcg$  vertex in (a-c) is shown in Fig.1.

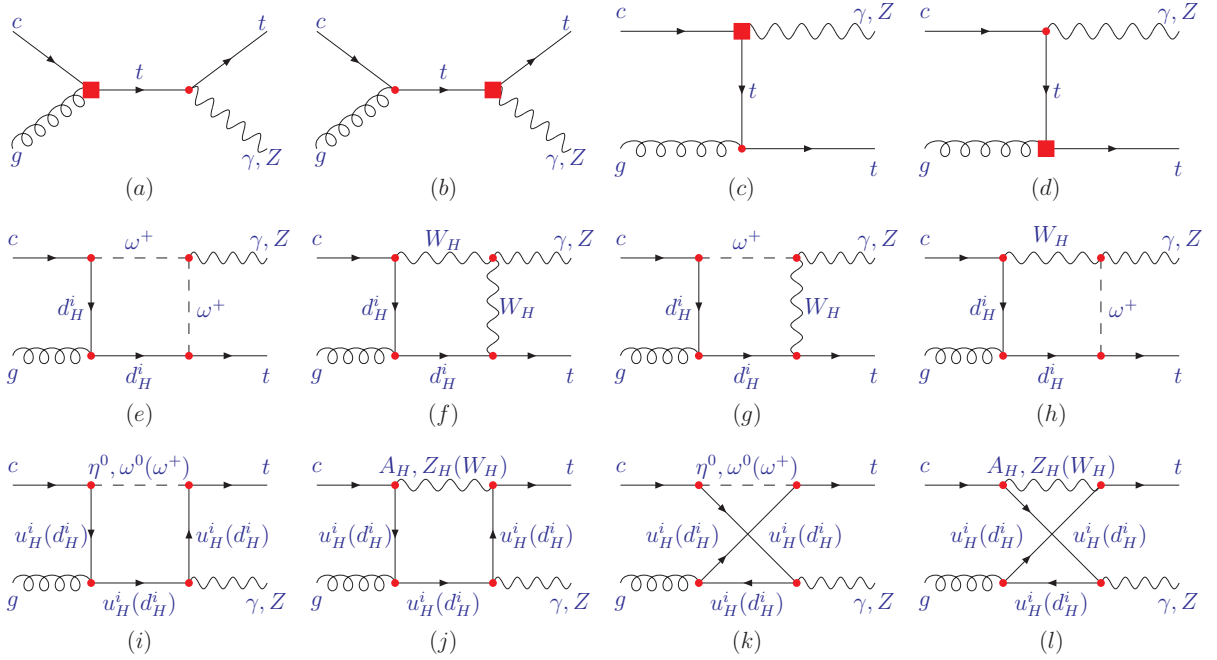


FIG. 3: Feynman diagrams for  $cg \rightarrow tV (V = \gamma, Z)$  at one-loop level in the LHT model. The loop-induced  $tcV$  vertex in (a-d) is shown in Fig.1.

in the matrices  $V_{H_u}$  and  $V_{H_d}$ . For the scale  $f$ , its value may be as low as 500 GeV [21]. For the mirror quark masses, from Eq.(4) we get  $m_{u_H^i} = m_{d_H^i}$  at  $\mathcal{O}(v/f)$  and further we assume

$$m_{u_H^1} = m_{u_H^2} = m_{d_H^1} = m_{d_H^2} \equiv m_{12}, \quad m_{u_H^3} = m_{d_H^3} \equiv m_3. \quad (6)$$

For the matrices  $V_{H_u}$  and  $V_{H_d}$ , considering the constraints in [9], we follow [13] to consider

two scenarios:

- (I)  $V_{H_d} = 1$ ,  $V_{H_u} = V_{CKM}^\dagger$ . In this scenario, the constraints on the mass spectrum of the mirror fermions can be relaxed [9]. The decay branching ratios in this scenario are

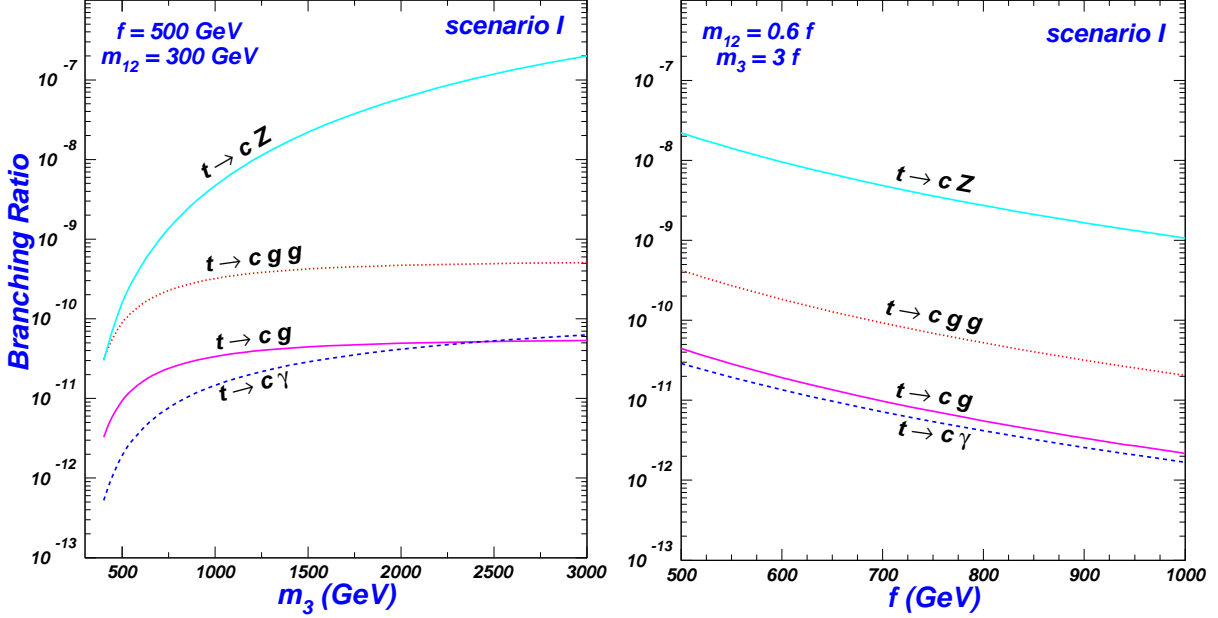


FIG. 4: The branching ratios of the top-quark FCNC decays in scenario I.

plotted in Fig. 4, where we fixed  $m_{12} = 300$  GeV and  $f = 500$  GeV for the left frame while for the right frame we assumed  $m_{12} = 0.6f$  and  $m_3 = 3f$  ( which corresponds to fixing the Yukawa couplings  $\kappa_{q^i}$  in Eq. 4).

- (II)  $s_{23}^d = 1/\sqrt{2}$ ,  $s_{12}^d = s_{13}^d = 0$ ,  $\delta_{12}^d = \delta_{23}^d = \delta_{13}^d = 0$ . In this scenario the  $D$ -meson system can give strong constraints on the relevant parameters [9]. Considering these constraints, we fixed  $f = 1000$  GeV and  $m_{12} = 500$  GeV for the results shown in the left frame of Fig. 5. In the right frame of Fig. 5 we show the results as a function of the scale  $f$  under the assumption  $m_{12} = 0.5f$  and  $m_3 = 1.2f$ .

As shown in the left frames in Figs. 4 and 5, the branching ratios increase with the mass of the third generation mirror fermions. The reason is that the decays are enhanced by the large mass splitting  $m_3 - m_{12}$ , which increases as  $m_3$  gets large since we fixed the value of  $m_{12}$ . From our numerical calculation we found that the contribution of each Feynman diagram in Fig. 1 increases drastically with  $m_3$ , but there is a strong cancellation between different diagrams for the decays  $t \rightarrow cg, c\gamma, cgg$ . For the decay  $t \rightarrow cZ$ , such a cancellation is weak because of the left-over divergence. So the enhancement with  $m_3$  is rapid for  $t \rightarrow cZ$

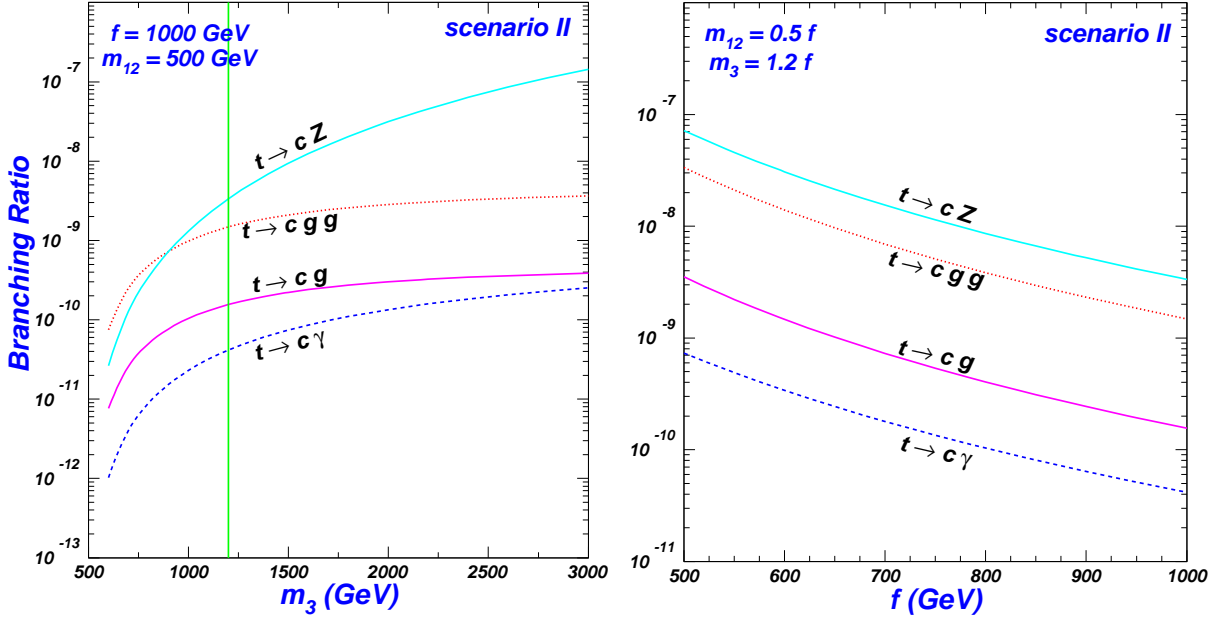


FIG. 5: The branching ratios of the top-quark FCNC decays in scenario II. The vertical line in the left frame is the upper bound on  $m_3$  from [9].

but mild for other decay modes. As shown in the right frames in Figs. 4 and 5, the branching ratios drop as the scale  $f$  (together with  $m_{12}$  and  $m_3$ ) gets large, showing the decoupling behavior of the scale  $f$  in the FCNC top quark decays.

From Figs. 4 and 5 we see that the branching ratio of  $t \rightarrow cgg$  is larger than that of  $t \rightarrow cg$ . Such a feature was also found in the SM [8] and the minimal supersymmetric model [15], and the reason is explained in the literature [15]. Another peculiar and unexpected phenomenon is that the branching ratio of  $t \rightarrow cZ$  is the largest. This is unique to the LHT model. The reason is that, unlike other decay modes,  $t \rightarrow cZ$  is special since it has the left-over divergence and is sensitive to the cut-off scale.

Now we turn to the top-quark FCNC productions at the LHC and present some numerical results. In our calculations we use CTEQ6L [22] for parton distributions, with the renormalization scale  $\mu_R$  and factorization scale  $\mu_F$  chosen to be  $\mu_R = \mu_F = m_t$ . In the following we use the parton processes to label the corresponding hadronic processes and all the cross sections displayed in our numerical results are the hadronic cross sections. Also, we take into account the charge conjugate channel for each process.

The cross sections are plotted in Figs. 6 and 7 for scenario I and II, respectively. The behavior of the curves is similar to those in Figs. 4 and 5, i.e., increase with  $m_3$  and decrease



with the scale  $f$ . Also, similar to the decay  $t \rightarrow cZ$ , the production rate of  $cg \rightarrow tZ$  increases rapidly with  $m_3$  because of its left-over divergence at  $\mathcal{O}(v^2/f^2)$ .

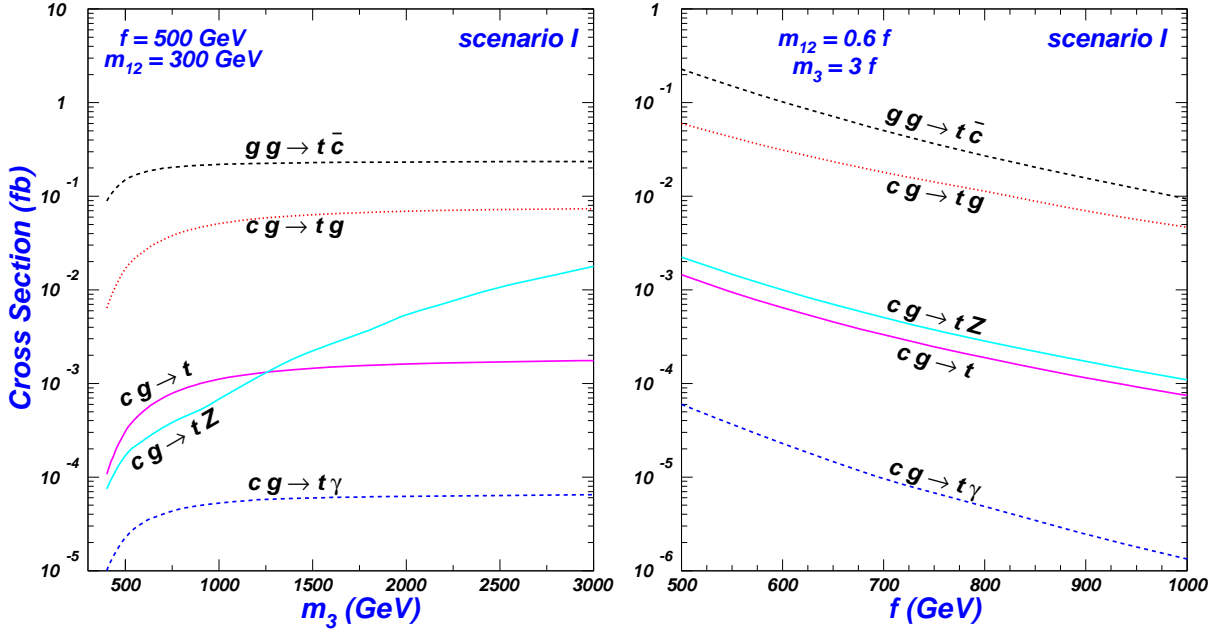


FIG. 6: The hadronic cross sections of FCNC top-quark productions in scenario I.

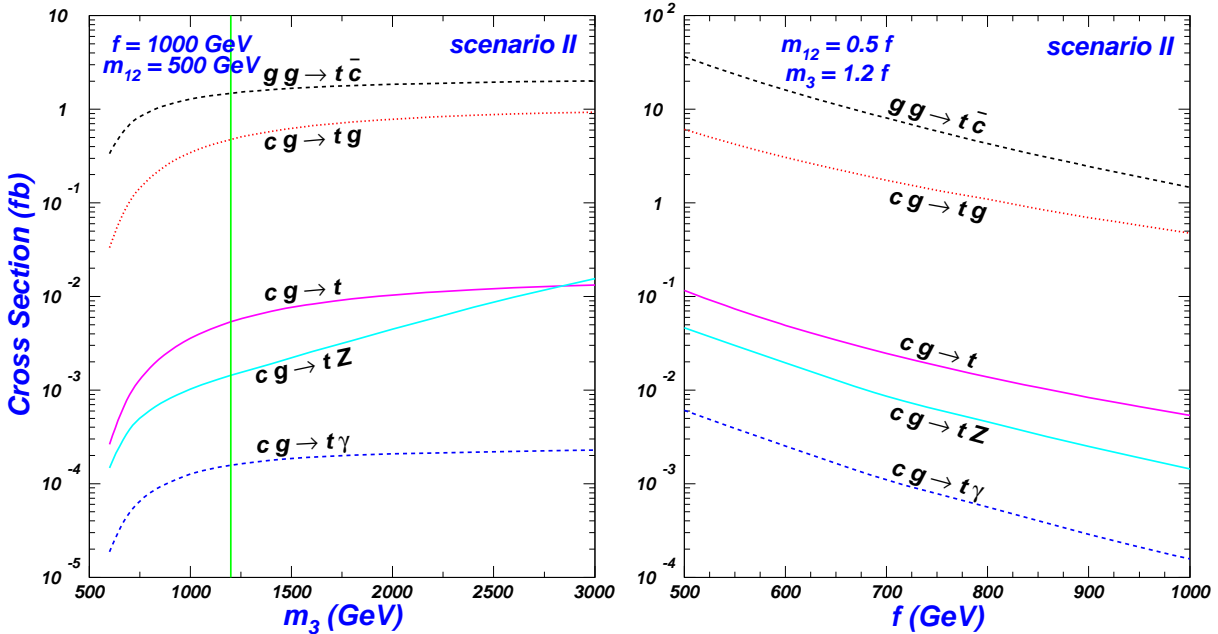


FIG. 7: The hadronic cross sections of FCNC top-quark productions in scenario II. The vertical line in the left frame is the upper bound on  $m_3$  from [9].

For the top FCNC decays, the LHC sensitivity with an integrated luminosity of  $100 \text{ fb}^{-1}$  is about  $10^{-5}$  for  $t \rightarrow c\gamma$  and  $t \rightarrow cZ$  [23] while for  $t \rightarrow cg$  and  $t \rightarrow cgg$  the sensitivity may

be much worse [24]. From Figs. 4 and 5 we see that the decay branching ratios are below  $10^{-7}$  and thus are not accessible at the LHC.

For the top FCNC productions, the LHC sensitivity is at pb level for  $cg \rightarrow t$ ,  $gg \rightarrow t\bar{c}$  and  $cg \rightarrow tg$  while at fb level for  $cg \rightarrow tZ$  and  $cg \rightarrow t\gamma$  [25]. From Figs. 6 and 7 we see that the the top FCNC productions in the LHT model are not accessible at the LHC.

Therefore, we conclude that although the LHT model can enhance the top quark FCNC processes relative to the SM predictions, its contributions are not large enough to be accessible at the LHC. This is in contrast to the topcolor-assisted technicolor models which give exceedingly large contributions above the LHC sensitivity [16]. The minimal supersymmetric model with R-parity conservation gives quite mild contributions to these FCNC processes of the top quark and only a couple of channels can marginally reach the LHC sensitivity in a tiny part of the parameter space [15]. If R-parity is violated, then the minimal supersymmetric model can give large contributions [15]. So, if the top quark properties are proved to be SM-like at the LHC and hence the top FCNC processes are not observed, the topcolor-assisted technicolor models and the R-parity violation in supersymmetric models will be severely constrained, while the R-conserving minimal supersymmetric model will be very mildly constrained and the LHT model will not be constrained.

Note that in [13] the LHT contributions to some FCNC top decay processes were found to be quite large. Unfortunately, our calculations cannot reproduce such large effects. Our results indicate that the LHT model does not cause flavor problem for the top quark sector.

#### IV. CONCLUSIONS

In the littlest Higgs model with T-parity the T-odd mirror quarks have flavor-changing couplings with the Standard Model quarks and may enhance the FCNC top quark interactions. We performed a comprehensive study for the contributions of these mirror fermions to various top quark FCNC decays and productions at the LHC. We found that although these FCNC processes can be greatly enhanced by the contributions of the mirror quarks, they are hardly accessible at the LHC. Therefore, this model may not cause the FCNC problem in the top quark sector if the top quark property is proved to be SM-like at the LHC.

## Acknowledgement

This work was supported by the National Natural Science Foundation of China (NNSFC) under Nos. 10821504, 10725526 and 10635030.

## APPENDIX A: THE AMPLITUDES OF $t \rightarrow cg$ AND $t \rightarrow cgg$ IN LHT

The amplitudes for various top FCNC processes are complicated and lengthy. Here, we only take  $t \rightarrow cg$  and  $t \rightarrow cgg$  for examples. The amplitude of  $t \rightarrow cg$  is given by

$$\mathcal{M} = \frac{ig_s T^a}{16\pi^2} \bar{u}_c(p_2) [(L_1 q^\mu + L_2 p_1^\mu + L_3 \gamma^\mu) P_L + (R_1 q^\mu + R_2 p_1^\mu + R_3 \gamma^\mu) P_R] u_t(p_1) \epsilon_\mu(q, \lambda), \quad (\text{A1})$$

where  $p_1, p_2$ , and  $q$  are the real momenta of top quark, charm quark and gluon respectively,  $\epsilon_\mu(q, \lambda)$  is the polarization vector of the gluon,  $P_{L,R} = (1 \mp \gamma_5)/2$ ,  $T^a$  are the generators of  $SU(3)_C$ . The factors  $L_i, R_i (i = 1, 2, 3)$  are the LHT contributions from the diagrams in Fig. 1, which include the scalar parts  $(L_i)_S, (R_i)_S$  and vector parts  $(L_i)_V, (R_i)_V$ . The scalar parts are given by

$$(L_1)_S = -2m_c b_2 a_3 (C_{21} + C_{11}) + 2m_t a_2 b_3 (C_{23} + C_{12}) + 2m_f a_2 a_3 (C_{11} + C_0), \quad (\text{A2})$$

$$(L_2)_S = 2m_c b_2 a_3 (C_{21} + C_{11} - C_{23} - C_{12}) + 2m_t a_2 b_3 (C_{22} - C_{23}) \\ + 2m_f a_2 a_3 (C_{12} - C_{11} - C_0), \quad (\text{A3})$$

$$(L_3)_S = b_2 a_3 [m_c^2 (C_{23} + C_{12} - C_{21} - C_{11}) + m_t^2 (C_{23} - C_{22}) + 1/2 - 2C_{24}] \\ + m_c m_t a_2 b_3 (C_{12} - C_{11}) + m_f (m_t b_2 b_3 + m_c a_2 a_3 + m_f b_2 a_3) C_0 \\ + \frac{1}{m_t^2 - m_c^2} \{ b_2 a_3 [m_t^2 (B_0(p_1) + B_1(p_1)) - m_c^2 (B_0(p_2) + B_1(p_2))] \\ + a_2 b_3 m_c m_t (B_0(p_1) + B_1(p_1) - B_0(p_2) - B_1(p_2)) \\ + b_2 b_3 m_f m_t (B_0(p_1) - B_0(p_2)) + a_2 a_3 m_f m_c (B_0(p_1) - B_0(p_2)) \}, \quad (\text{A4})$$

$$(R_1)_S = 2m_t b_2 a_3 (C_{23} + C_{12}) - 2m_c a_2 b_3 (C_{21} + C_{11}) + 2m_f b_2 b_3 (C_{11} + C_0), \quad (\text{A5})$$

$$(R_2)_S = 2m_t b_2 a_3 (C_{22} - C_{23}) + 2m_c a_2 b_3 (C_{21} + C_{11} - C_{23} - C_{12}) \\ + 2m_f b_2 b_3 (C_{12} - C_{11} - C_0), \quad (\text{A6})$$

$$\begin{aligned}
(R_3)_S &= a_2 b_3 [m_c^2 (C_{23} + C_{12} - C_{21} - C_{11}) + m_t^2 (C_{23} - C_{22}) + 1/2 - 2C_{24}] \\
&\quad + b_2 a_3 m_c m_t (C_{12} - C_{11}) + m_f (b_2 b_3 m_c + a_2 a_3 m_t + a_2 b_3 m_f) C_0 \\
&\quad + \frac{1}{m_t^2 - m_c^2} \{ a_2 b_3 [m_t^2 (B_0(p_1) + B_1(p_1)) - m_c^2 (B_0(p_2) + B_1(p_2))] \\
&\quad + b_2 a_3 m_c m_t (B_0(p_1) + B_1(p_1) - B_0(p_2) - B_1(p_2)) \\
&\quad + a_2 a_3 m_f m_t (B_0(p_1) - B_0(p_2)) + b_2 b_3 m_f m_c (B_0(p_1) - B_0(p_2)) \} \quad (A7)
\end{aligned}$$

where  $C_{ij}(-p_2, p_1, m_f, m_S, m_f)$ ,  $B_i(p_1)(p_1, m_S, m_f)$  and  $B_i(p_2)(p_2, m_S, m_f)$  are the loop functions [18]. The vector parts are given by

$$(L_1)_V = 4m_c c_2 c_3 (C_{21} + C_{11}), \quad (A8)$$

$$(L_2)_V = 4m_c c_2 c_3 (C_{23} - C_{21}), \quad (A9)$$

$$\begin{aligned}
(L_3)_V &= 2c_2 c_3 [m_c^2 (C_{21} - C_{23}) + m_t^2 (C_{22} + C_{12} - C_{23} - C_{11}) - m_f^2 C_0 + 2C_{24} - 1] \\
&\quad + \frac{c_2 c_3}{m_t^2 - m_c^2} [m_c^2 (2B_0(p_2) + 2B_1(p_2) - 1) - m_t^2 (2B_0(p_1) + 2B_1(p_1) - 1)], \quad (A10)
\end{aligned}$$

$$(R_1)_V = -4m_t c_2 c_3 (C_{23} + C_{11}), \quad (A11)$$

$$(R_2)_V = 4m_t c_2 c_3 (C_{23} + C_{11} - C_{22} - C_{12}), \quad (A12)$$

$$(R_3)_V = 2c_2 c_3 m_c m_t (C_{12} - C_{11}) + \frac{2m_c m_t c_2 c_3}{m_t^2 - m_c^2} [B_0(p_2) + B_1(p_2) - B_0(p_1) - B_1(p_1)] \quad (A13)$$

with  $C_{ij}(-p_2, p_1, m_f, m_V, m_f)$ ,  $B_i(p_1)(p_1, m_V, m_f)$  and  $B_i(p_2)(p_2, m_V, m_f)$ . Other relevant parameters are from

$$\begin{aligned}
S\bar{c}f &: a_2 P_L + b_2 P_R, & S\bar{f}t &: a_3 P_L + b_3 P_R, \\
V\bar{c}f &: i\gamma^\mu c_2 P_L, & V\bar{f}t &: i\gamma^\mu c_3 P_L, \quad (A14)
\end{aligned}$$

where  $V$  represents gauge bosons and  $S$  represents scalar particles. These couplings represent the five different classes of vertexes involved in our calculation. In each class of vertexes, the parameters,  $a_2$ ,  $b_2$ ,  $a_3$ ,  $b_3$ ,  $c_2$ ,  $c_3$ , take different values for the every concrete coupling, respectively. The analytic expressions of parameters are complicated at  $\mathcal{O}(v^2/f^2)$  and can be found in [11].

Now we give the amplitude of  $t \rightarrow cgg$ . The expressions of Fig.2(a-c) are simple and can be obtained straightforwardly from the effective vertex of  $tcg$ . For the box diagrams (d) and (e) in Fig.2, their expressions are given by

$$\mathcal{M}_d = -\frac{ig_s^2}{16\pi^2} T_{ij}^a T_{jk}^b \bar{u}_c(p_2) (a_2 P_L + b_2 P_R) S_{box} (a_3 P_L + b_3 P_R) u_t(p_1) \quad (A15)$$

$$\mathcal{M}_e = -\frac{ig_s^2}{16\pi^2} T_{ij}^a T_{jk}^b \bar{u}_c(p_2) \gamma^\rho c_2 P_L S_{box} c_3 P_L \gamma_\rho u_t(p_1) \quad (A16)$$

where

$$\begin{aligned}
S_{box} = & D_{\alpha\beta\gamma}\gamma^\alpha \epsilon_1^*\gamma^\beta \epsilon_2^*\gamma^\gamma + D_{\alpha\beta}[m_f\gamma^\alpha \epsilon_1^*\gamma^\beta \epsilon_2^* + \gamma^\alpha \epsilon_1^*(m_f - \not{q}_2) \epsilon_2^*\gamma^\beta \\
& + (m_f - \not{\phi}_s\text{lash} + \not{p}'_2) \epsilon_1^*\gamma^\alpha \epsilon_2^*\gamma^\beta] + D_\alpha[m_f(m_f - \not{\phi}_s\text{lash} + \not{p}'_2) \epsilon_1^*\gamma^\alpha \epsilon_2^* \\
& + (m_f - \not{\phi}_s\text{lash} + \not{p}'_2) \epsilon_1^*(m_f - \not{q}_2) \epsilon_2^*\gamma^\alpha + m_f\gamma^\alpha \epsilon_1^*(m_f - \not{q}_2) \epsilon_2^*] \\
& + D_0 m_f(m_f - \not{\phi}_s\text{lash} + \not{p}'_2) \epsilon_1^*(m_f - \not{q}_2) \epsilon_2^* \tag{A17}
\end{aligned}$$

with  $D(-p_2, p_1, q_1, q_2, m_f, m_{S(V)}, m_f, m_f)$  being 4-point loop function [18],  $p_1$ ,  $p_2$ ,  $q_1$  and  $q_2$  being respectively the momenta of top quark, charm quark and two emitting gluons, and  $\epsilon_1$  and  $\epsilon_2$  are the polarization vectors of gluons.

- 
- [1] N. Arkani-Hamed, A. G. Cohen and H. Georgi, Phys. Lett. B **513**, 232 (2001); N. Arkani-Hamed, *et al.*, JHEP **0208**, 020 (2002); JHEP **0208**, 021 (2002); I. Low, W. Skiba and D. Smith, Phys. Rev. D **66**, 072001 (2002); D. E. Kaplan and M. Schmaltz, JHEP **0310**, 039 (2003).
- [2] N. Arkani-Hamed, A. G. Cohen, E. Katz, A. E. Nelson, JHEP **0207**, 034 (2002); S. Chang, JHEP **0312**, 057 (2003); T. Han, H. E. Logan, B. McElrath and L. T. Wang, Phys. Rev. D **67**, 095004 (2003); M. Schmaltz, D. Tucker-smith, Ann. Rev. Nucl. Part. Sci. **55**, 229 (2005).
- [3] C. Csaki, *et al.*, Phys. Rev. D **67**, 115002 (2003); Phys. Rev. D **68**, 035009 (2003); J. L. Hewett, F. J. Petriello, T. G. Rizzo, JHEP **0310**, 062 (2003); M. C. Chen, S. Dawson, Phys. Rev. D **70**, 015003 (2004); M. C. Chen, *et al.*, Mod. Phys. Lett. A **21**, 621 (2006); W. Kilian, J. Reuter, Phys. Rev. D **70**, 015004 (2004).
- [4] G. Marandella, C. Schappacher and A. Strumia, Phys. Rev. D **72**, 035041 (2005).
- [5] H. C. Cheng and I. Low, JHEP **0309**, 051 (2003); JHEP **0408**, 061 (2004); I. Low, JHEP **0410**, 067 (2004); J. Hubisz, P. Meade, Phys. Rev. D **71**, 035016 (2005).
- [6] C. R. Chen, K. Tobe, C. P. Yuan, Phys. Lett. B **640**, 263 (2006); K. Hsieh, C. P. Yuan, Phys. Rev. D **78**, 053006 (2008). C. O. Dib, R. Rosenfeld, A. Zerwekh, JHEP **0605**, 074 (2006); L. Wang *et al.*, Phys. Rev. D **76**, 017702 (2007); Phys. Rev. D **75**, 074006 (2007); Phys. Rev. D **77**, 015020 (2008) R. S. Hundi, B. Mukhopadhyaya, A. Nyffeler, Phys. Lett. B **649**, 280 (2007); R. S. Hundi, B. Mukhopadhyaya, A. Nyffeler, Phys. Lett. B **649**, 280 (2007); C. R. Chen, K. Tobe, C. P. Yuan, Phys. Lett. B **640**, 263 (2006).

- [7] For top quark reviews, see, e.g., W. Bernreuther, J. Phys. G **35**, 083001,(2008) D. Chakraborty, J. Konigsberg, D. Rainwater, Ann. Rev. Nucl. Part. Sci. **53**, 301 (2003); E. H. Simmons, hep-ph/0211335; C.-P. Yuan, hep-ph/0203088; S. Willenbrock, hep-ph/0211067; M. Beneke *et al.*, hep-ph/0003033; T. Han, arXiv:0804.3178; For model-independent new physics in top quark, see, e.g., C. T. Hill, S. J. Parke, Phys. Rev. D **49**, 4454 (1994); K. Whisnant, *et al.*, Phys. Rev. D **56**, 467 (1997); J. M. Yang, B.-L. Young, Phys. Rev. D **56**, 5907 (1997); K. Hikasa, *et al.*, Phys. Rev. D **58**, 114003 (1998); J. A. Aguilar-Saavedra, arXiv:0811.3842.
- [8] For top FCNC in the SM, see, G. Eilam, J. L. Hewett, A. Soni, Phys. Rev. D **44**, 1473 (1991); B. Mele, S. Petrarca, A. Soddu, Phys. Lett. B **435**, 401 (1998); A. Cordero-Cid *et al.*, Phys. Rev. D **73**, 094005 (2006); G. Eilam, M. Frank, I. Turan, Phys. Rev. D **73**, 053011 (2006).
- [9] J. Hubisz, S. J. Lee, G. Paz, JHEP **0606**, 041, 2006.
- [10] M. Blanke, *et al.*, arXiv:0805.4393.
- [11] M. Blanke, *et al.*, JHEP **0701**, 066 (2007); JHEP **0612**, 003 (2006).
- [12] X. F. Han, L. Wang and J. M. Yang, Phys. Rev. D **78**, 075017 (2008); C. X. Yue, J. Y. Liu and S. H. Zhu, Phys. Rev. D **78**, 095006 (2008).
- [13] H. S. Hou, Phys. Rev. D **75**, 094010 (2007).
- [14] X. Wang, Y. Zhang, H. Jin and Y. Xi, Nucl. Phys. B **810**, 226 (2009).
- [15] C. S. Li, R. J. Oakes, J. M. Yang, Phys. Rev. D **49**, 293 (1994); G. Couture, C. Hamzaoui, H. Konig, Phys. Rev. D **52**, 1713 (1995); J. L. Lopez, D. V. Nanopoulos, R. Rangarajan, Phys. Rev. D **56**, 3100 (1997); G. M. de Divitiis, R. Petronzio, L. Silvestrini, Nucl. Phys. B **504**, 45 (1997); J. M. Yang, B.-L. Young, X. Zhang, Phys. Rev. D **58**, 055001 (1998); G. Eilam, *et al.*, Phys. Lett. B **510**, 227 (2001); C. S. Li, L. L. Yang, L. G. Jin, Phys. Lett. B **599**, 92 (2004); M. Frank, I. Turan, Phys. Rev. D **74**, 073014 (2006); J. M. Yang, C. S. Li, Phys. Rev. D **49**, 3412 (1994); J. Guasch, J. Sola, Nucl. Phys. B **562**, 3 (1999); J. Guasch, *et al.*, hep-ph/0601218; J. M. Yang, Annals Phys. **316**, 529 (2005); Int. J. Mod. Phys. A23, 3343 (2008); J. Cao, *et al.*, Nucl. Phys. B **651**, 87 (2003); Phys. Rev. D **74**, 031701 (2006); Phys. Rev. D **75**, 075021 (2007); Phys. Rev. D **79**, 054003 (2009).
- [16] H. J. He and C. P. Yuan, Phys. Rev. Lett. **83**, 28(1999); G. Burdman, Phys. Rev. Lett. **83**,2888(1999); X. L. Wang *et al.*, Phys. Rev. D **50**, 5781 (1994); J. Cao, *et al.*, Phys. Rev. D **67**, 071701 (2003); Phys. Rev. D **70**, 114035 (2004); Eur. Phys. Jour. C **41**, 381 (2005); Phys. Rev. D **76**, 014004 (2007); H. J. Zhang, Phys. Rev. D **77**, 057501 (2008); G. L. Liu, H.

- J. Zhang, Chin. Phys. C 32, 597 (2008) [arXiv:0708.1553]; G. L. Liu, arXiv:0903.2619.
- [17] M. Blanke, *et al.*, Phys. Lett. B **646**, 253 (2007).
- [18] G. 't Hooft and M. J. G. Veltman, Nucl. Phys. B **153**, 365 (1979).
- [19] T. Hahn and M. Perez-Victoria, Computl. Phys. Commun. **118**, 153 (1999); T. Hahn, Nucl. Phys. Proc. Suppl. **135**, 333 (2004).
- [20] T. Goto, Y. Okada and Y. Yamamoto, Phys. Lett. B **670**, 378 (2009).
- [21] J. Hubisz, P. Meade, A. Noble and M. Perelstein, JHEP **01**, 135 (2006).
- [22] J. Pumplin, *et al.*, JHEP **0602**, 032 (2006).
- [23] T. Han, K. Whisnant, B. L. Young and X. Zhang, Phys. Rev. D **55**, 7241 (1997). M. Beneke, *et al.*, hep-ph/0003033; T. Han, R. D. Peccei and X. Zhang, Nucl. Phys. B **454**, 527 (1995); L. Chikovani and T. Djobava, hep-ex/0205016.
- [24] J. A. Aguilar-Saavedra, Acta Phys. Polon. B **35**, 2695 (2004).
- [25] M. Hosch, K. Whisnant and B. L. Young, Phys. Rev. D **56**, 5725 (1997); T. Stelzer, Z. Sullivan and S. Willenbrock, Phys. Rev. D **58**, 094021 (1998); T. Han, *et al.*, Phys. Rev. D **58**, 073008 (1998); F. del Aguila and J. A. Aguilar-Saavedra, Nucl. Phys. B **576**, 56 (2000).